A STUDY OF WAVE AMPLIFICATION IN THE VENETIAN HARBOR OF CHANIA, CRETE

Nikolaos Maravelakis[1], Nikos Kalligeris[2], Patrick J. Lynett[2], Vassilios Skanavis[2] and Costas E. Synolakis[1,2]

We studied resonance in the Venetian Port of Chania, a 14th century historic monument, which frequently exhibits large wave motions in its basin with flooding of its docks. We measured time histories of surface elevation and currents off the harbor for a period of two years and also measured wave elevations at one location inside the Port. Offshore, we recorded maximum H_s= 4.1m with T_s =9.2s. We employed a Boussinesq-type model *COULWAVE* to explore resonance and determined the resonant frequencies for the entire basin. We also examined the effect of a past proposed breakwater extension design on the resonant frequencies and respective modes. We conclude that the overtopping observed under storm conditions may not be the result of harbor resonance but the little protection of the existing breakwater sheltering the entrance.

Keywords: harbor resonance; numerical modeling; Boussinesq

INTRODUCTION

The island of Crete, Greece is a popular tourist destination in the Eastern Mediterranean. Crete is estimated to produce approximately 1/5 of the GDP of Greece just in the summer months. The municipality of Chania in Western Crete ranks second among all Greek tourist destinations and depends on its waterfront, which is estimated to generate about 90% of its tourist income.

The coastal zone of Chania has been subjected to multiple human interventions that have degraded its waterfront. Coastal roads, seawalls and small fishing harbors are examples of poorly planned anthropogenic interference, also observed in other coastal cities in Crete (Synolakis et *al.* 2008).

Amongst other coastal engineering-related issues the municipality faces the lack of an organized Marina that offers safe shelter in wintertime. The only available local harbor for cruising boats, used by locals and visitors is the picturesque Venetian harbor, the very symbol of the city of Chania. Although a visually attractive location for docking, the harbor, first built in the 14th century, is small. A section of the harbor remains unprotected from northern storm waves. During winter storms, offshore waves reaching H_s = 4.5m (trough to crest) enter the western harbor basin overtopping the docks and flooding businesses around its parameter. The harbor is a national historic monument, and any intervention has to be approved by numerous local agencies and national authorities, which usually do not agree on what is needed, a situation exacerbated by lack of world class experience with port design.

Here, we examine the contribution of harbor resonance in the excitation of the Venetian harbor basin during typical winter storms. Harbors are known to be excited by long waves (Lepelletier and Raichlen, 1987; Okihiro et *al*., 1993; Okihiro and Guza, 1996). We deployed an offshore directional wave measuring system since 2010, recording the offshore incident wave field, and a bottom pressure gauge inside the port to measure the surface elevation in the harbor basin. Long-wave forcing and harbor resonance are factors that have not been considered in the two earlier studies that looked into improving the protection of the docks. Infra-gravity waves released by nonlinear wave-wave interaction in the surf zone provide the long wave forcing, which can be amplified around the resonant frequencies of the harbor. We identify these frequencies using the Boussinesq-type numerical model *COULWAVE* (Lynett, 2002; Lynett and Liu 2004).

THE HARBOR

Crete has been a commercial center for the Easter Mediterranean for at least four millennia, and Chania has been continuously inhabited at least back to Minoan times. The Venetian Harbor of Chania was built in the 14th century and is considered a monument of great importance for Crete. It was constructed in a natural rocky shelter on the northern shore of the island, on the east end of the bay of Chania to serve the homonymous Venetian city.

The most frequent wind directions, as recorded from a local weather station, are from the W and WNW. However, it is the strong northern storms with wind speeds up to 40knots with the longest fetch that affect the harbor the most (Fig. 1b). The location and geometry of the natural harbor layout do not offer protection from the prevailing northern wave storms. For that reason, and due to siltation issues, it had been periodically abandoned from maintenance and use (before modern times) and it has been left up to this day without an effective entrance protection scheme. This is not unusual for ancient ports,

[1] Department of Environmental Engineering, Technical University of Crete, Chania, Crete, 73100, Greece
[2] Department of Civil and Environmental Engineering, University of Southern California, 3620 S. Vermont Avenue, Los Angeles, California, 90089, USA

Alexandria is another example of a port that was abandoned presumably following a large natural disaster, and rebuilt decades or centuries later.

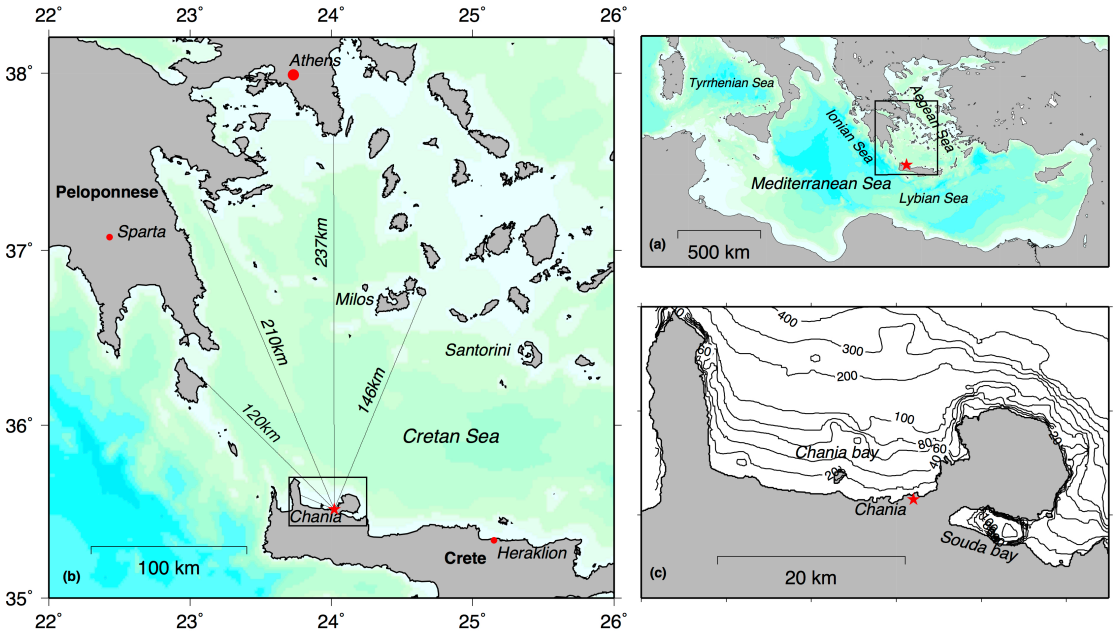

Figure 1. Geographical location of Chania city. (a) Location with respect to the Mediterranean basin. (b) Fetch distances to the harbor: NW, NNW, N, NNE. (c) Bathymetry contours in Chania bay. Rectangle in (a) denotes the boundaries of (b), and rectangle in (b) denotes the boundaries of (c).

The harbor has gone through several changes in its layout throughout its lifespan (Fig. 2). The modifications have been mostly landfills to create docks and did not address the issue of protection from the storm waves. In 1986 and 1992, two studies focused on the design of a low crested offshore breakwater near the harbor entrance. The proposed breakwater of the first study was partially constructed while the second design (extension of the existing one) never materialized. The existing ~100m breakwater has a rubble mound core and an armoring layer of RC tetrapods many of which have been displaced by storm waves rendering the breakwater from low crested to partially submerged. One of us observed during construction that the crane operators had no special training, and placed the units hastily and as convenient. The location and orientation of the breakwater offer some protection only from NW waves, and are entirely ineffective during northern wave storms.

Presently, the harbor occupies a total water surface of 108000m^2 and is divided in two basins (east and west) by two jetties. The eastern basin of the harbor measures 400x125m with an average depth of ~3m and is used by recreational vessels and fishing boats throughout the year. In the western basin (320x180m with ~4m average depth), small cruising boats lay up in the summer only. Its perimeter is occupied by restaurants and is essentially functional half of the year because of the severe overtopping and flooding of the dock from the storm waves. The boats enter the harbor through the ~90m wide main harbor entrance, which lies over a natural submarine canyon. There is another 4m wide entrance cutting through the northern breakwater and it leads to the eastern basin, allowing for the basin water to circulate. The perimeter of the harbor consists mostly of vertical reflective walls, with the exception of some locations in the western basin, where boulders have been placed in front of the docks by the port authority, in a desperate effort to reduce overtopping and scouring.

FIELD MEASUREMENTS

There are no published near shore wave measurements in Crete. Some short-time measurements of the order of a few days are believed to have been made to supplement design of modifications of or plans for structures, but there are no available long-term data. Design of structures in contemporary Greek practice relies on wave hind casting using mainly the SMB method.

Figure 2. Evolution of the Venetian harbor of Chania. The dates of the gravures, clockwise from top left, correspond to: i) The second half of the 16th century, ii) between 1618-1668, and iii) 1645. Satellite image at the bottom left shows the harbor as it is today (source: Google Earth).

In the absence of wave measurements in the broader study area, in December 2010, the Coastal Engineering Group of the Technical University of Crete initiated a concerted effort to continuously record waves and currents in the Bay of Chania. Two *AWAC* 600kHz instruments (Nortek International) measuring current profiles and direction-resolved surface elevation have been deployed at 20-25m depth in various locations in the Bay with one instrument always just offshore the harbor. The *AWAC*s were set to record 2400 samples at 2Hz (20 minutes), every hour through the Acoustic Surface Tracking method (AST). With the exception of the period between 10/03/2012 – 26/10/2012, when due to technical difficulties there is a gap in our data, the dataset is otherwise continuous. The results presented here are from the *AWAC* deployed just offshore from the harbor entrance (Fig. 3).

For the study of the wave climate in the harbor basin under storm conditions, we deployed a *TWR-2050* bottom pressure gauge approximately in the middle of the western basin at 5m depth (Fig. 3). The *TWR* has been recording for different sampling periods and at different sampling rates for the storm events it was deployed. The deployment location at the harbor seafloor and the sampling settings were chosen to optimally collect data about wave attenuation and are not ideal for capturing all the resonant modes of the harbor basin. We are planning to revise the locations and sampling settings of the instruments based on the numerical modeling results of this study to extract more suitable data for the study of long waves.

Details about the measurements regarding the location offshore the old harbor are given in the wave-rose of Fig. 3 and Fig. 4. It has been observed that storm events with $H_s > 3$m cause significant overtopping and flooding of the harbor. From Table 1 it is seen that events with $H_s > 3$m have periods between $7\text{s} < T_s < 9\text{s}$, while the direction of these waves is mainly northerly.

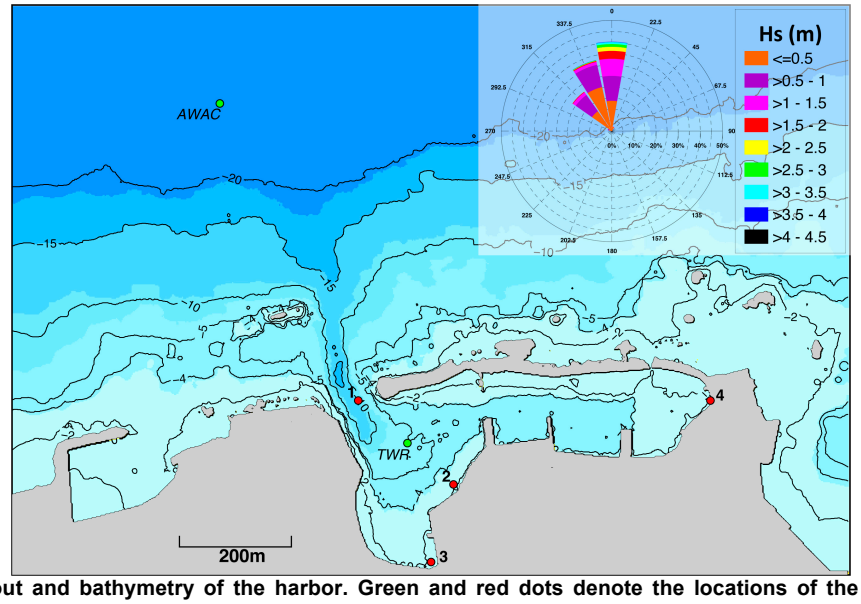

Figure 3. Layout and bathymetry of the harbor. Green and red dots denote the locations of the field and numerical wave gauges respectively. The inlet in the top right corner shows the offshore wave rose.

In the present paper, we focus on field measurements during storm events. An example of measurements from both locations is shown at Fig. 4. From top to bottom, the first graph shows the significant wave height (H_s) offshore and inside the harbor with the corresponding significant wave periods shown at the graph below. In the third graph, the wave heights offshore and inside the harbor are correlated, and at the fourth graph the amplification, i.e., the ratio between the wave height inside the harbor and offshore is given in as a function of the offshore significant wave period. In Fig. 5 we compare the energy density spectrograms offshore and inside the harbor for the same storm event on the 03/12/2013 with H_s = 4.1m and T_s = 9.2s (H_{max} in the same record was measured at 7.5m).

Table 1. Joint frequency table of significant period (T_s) and significant wave height (H_s).

Hs (m)	<=2	2-3	3-4	4-5	5-6	6-7	7-8	8-9	9-10	*Sum*
<=0.5	0.25	11.95	25.26	13.07	2.35	0.53	0.06	0.00	0.00	53.45
0.5-1	0.00	0.72	7.69	14.82	5.70	0.35	0.01	0.01	0.00	29.30
1-1.5	0.00	0.00	0.17	2.32	6.31	0.65	0.00	0.00	0.00	9.45
1.5-2	0.00	0.00	0.00	0.10	1.57	2.02	0.06	0.00	0.00	3.75
2-2.5	0.00	0.00	0.00	0.00	0.24	1.31	0.28	0.00	0.00	1.83
2.5-3	0.00	0.00	0.00	0.00	0.00	0.42	0.64	0.08	0.00	1.13
3-3.5	0.00	0.00	0.00	0.00	0.00	0.11	0.62	0.19	0.00	0.92
3.5-4	0.00	0.00	0.00	0.00	0.00	0.01	0.04	0.07	0.02	0.15
4-4.5	0.00	0.00	0.00	0.00	0.00	0.00	0.00	0.01	0.00	0.01
Sum	0.25	12.66	33.12	30.31	16.17	5.40	1.71	0.36	0.02	100

From the figure, it appears that during the most intense storms recorded, when offshore H_s > 3.5m, the H_s inside the harbor exceeds 1m, with 1.4m being the maximum value recorded. The offshore T_s exceeds 7s while in the harbor the corresponding T_s is about 1s less. For storms, the ratio between the H_s inside the harbor and offshore is around 0.3 for all periods. Comparing the spectrograms, the frequencies of high energy from offshore coincide with their equivalents inside. Also, the amplification of energy in the harbor at low frequencies (f < 0.05 Hz) is apparent.

Bathymetric data were collected using the single beam echo sounder *Sonar Mite* (Ohmex Instruments) to generate the high-resolution grid the numerical modeling necessitates. Soundings were coupled on board to differential GPS (*Hiper Pro*, Topcon) measurements. Topographic and shallow water relief was obtained using the GPS system and the two sets (bathymetric and topographic) were integrated to create a 2m cell-sized seamless grid (referenced at MWL). Fig. 3 shows the bathymetry which is cutoff at h = 20m to create the constant depth wave generation area for *COULWAVE*.

As a side note, the wave and current measurements were are also used to aid with studies of coastal resilience and beach erosion in Crete (Skanavis et *al*. 2014). Substandard coastal engineering practices and poor coastal zone management have exasperated the substantial erosion observed in most of Greece's beaches of value to the tourist industry. The Laboratory of Natural Hazards and Coastal Engineering at the Technical University of Crete has undertaken a substantial effort to educate local

authorities and the public on basic concepts of coastal resilience (Ewing et *al.*, 2008 and 2010; Foteinis and Synolakis, 2014). The focus is to underscore the importance of long-term quantitative measurements to near shore waves and currents as a necessary requirement for any future coastal engineering studies.

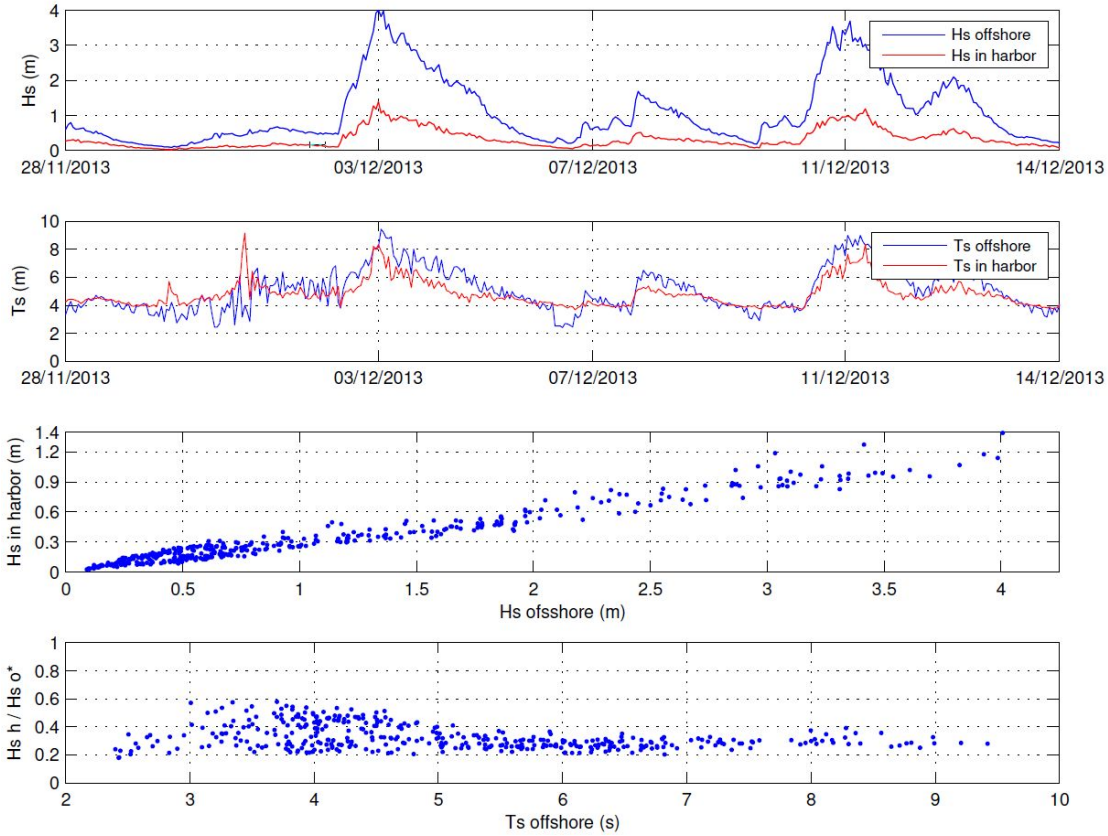

Figure 4. Comparison between significant wave height H_s and significant period T_s offshore (*AWAC*) and in the harbor (*TWR*).

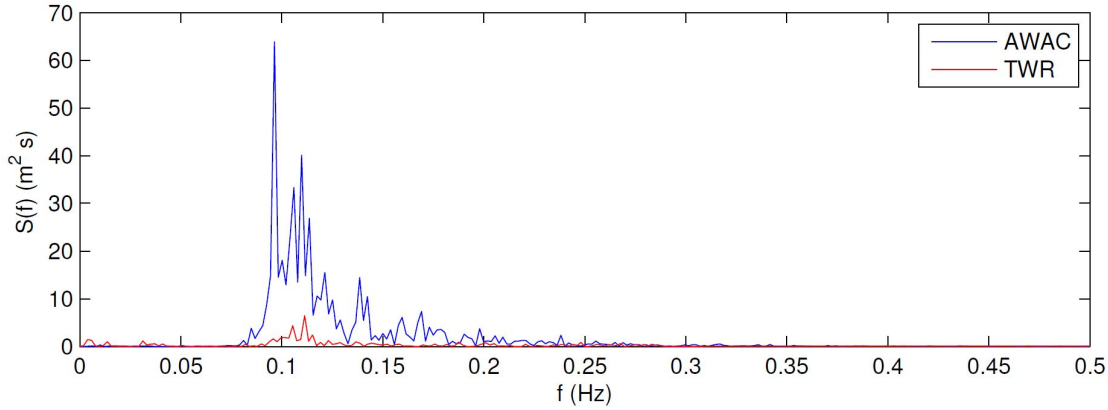

Figure 5. Comparison of offshore wave spectra (*AWAC*) and in the harbor (*TWR*) for a storm event on 03/12/2014.

NUMERICAL MODELING

In the absence of detailed harbor oscillation field measurements, we employ a Boussinesq-type model to study the response of the harbor under storm conditions. Typical models to study harbor resonance include mild-slope equation models (e.g. Berkhoff, 1972; Chen and Houston, 1987; Briggs et *al.* 2004) or Boussinesq-type equation models (e.g. Nwogu, 2000). Mild-slope models in their usual form are linear and accurately simulate wave propagation, refraction, diffraction and reflection at boundaries (in some models), as long as the mild-slope bathymetry approximation is not violated (~1/3

maximum slope). In harbor resonance studies, such models make it possible to obtain amplification factors for various frequencies; however, their linearity cannot model the release of infra-gravity waves in the surf zone using a realistic offshore spectrum. Also, in most mild-slope equation models, boundary conditions in the harbor basin are defined as either partially or totally reflective by using reflection coefficients, and not performing runup computations on real topography. Consequently, the estimation of resonant frequencies may be unreliable, if reflection coefficients are poorly estimated.

Boussinesq-type (BT) models offer a more accurate alternative for the study of harbor resonance. Although significantly more computationally demanding, BT models in their weakly non-linear (e.g. Peregrine, 1967; Nwogu, 1993; Kazolea et *al.* 2012; Kazolea et *al*. 2014) and fully non-linear (e.g. Wei et *al.*, 1995) forms are phase-resolving and can simulate non-linear wave-wave interaction. Therefore, there is no need for a priori assumptions on the long wave forcing the harbor is subjected to during a simulated storm event. Such models have been used successfully in the past to study resonance in harbors (e.g. Nwogu, 2000; Kofoed-Hansen et *al.*, 2005). More specifically, *COULWAVE* has been applied to study harbor oscillations at two Hawaiian harbors, showing reasonable agreement with previously published linear model results and field data (Douyere, 2003).

Here, we use the fully non-linear solver *COULWAVE*. The model solves the equations of Wei et *al.* (1995), evaluated at an arbitrary level (Nwogu, 1993), using a finite volume solver and regular grids. Energy is dissipated through bottom friction, through a Manning's friction term, while wave breaking through a transport-based breaking model. Boundary conditions allow runup computations on real topography, and outgoing waves are absorbed at the boundaries using appropriate sponge layers. Finally, the wave input is defined through a two-dimensional (frequency and azimuth) *TMA* spectrum (Bouws et *al.* 1985), which in our application corresponds to an idealized northern storm, among the ones recorded, with statistical parameters: H_s = 3.5m, T_p = 8.5s, γ = 3.3 and s_m = 80, defined at h = 20m offshore depth.

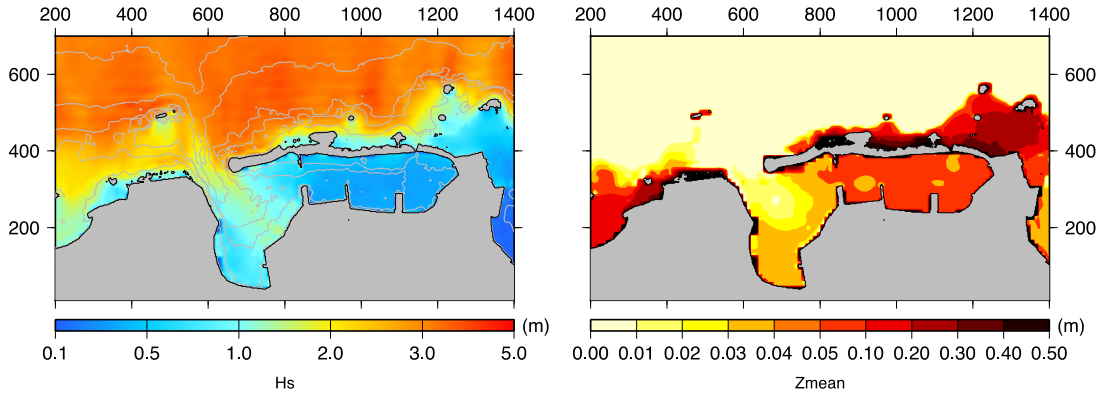

Figure 6. Maps showing the distribution of significant wave height H_s (left) and mean sea level z_{mean} (right) as extracted from the numerical simulation.

We ran the model for 200mins real time, and the first 20mins of the simulation were disregarded from processing, to allow the model to reach steady state. The simulation shows waves with significant height 1.5m traveling towards the quay of the western basin which experiences substantial overtopping during storms (see Fig. 6). Significant wave height is lower (~0.9m) at the southernmost tip of the western basin, which is another location frequently experiencing overtopping. However, the height of the quay at that point is just 60cm above MWL. Set-up is in the order of 3cm in the western basin, thus not contributing significantly to overtopping (see Fig. 6). The modeling results for H_s compare well with measurements from the pressure gauge in the harbor for similar offshore wave conditions (H_{smod} = 1.08m Vs H_{sTWR} = 1m).

Surface elevation time series in the harbor basin were stored in a 10m-spaced array (see Fig. 8) and the corresponding spectral amplitudes were computed using FFT. The raw power spectra in the infra-gravity (IG) frequency range (<0.05Hz), corresponding to four numerical gauges (for locations see Fig. 3) in the basin, are shown in Fig 6. The long simulation time results in a very small spectral frequency step $\Delta f \sim 10^{-4}$ (=1/T, where T is the sampling duration), which in turn produces discrete peaks around the resonant frequencies. The frequency at maximum spectral energy varies with location because of the spectral energy distribution of each resonant mode. Gauge 1, which is located close to the open boundary (harbor entrance), contains less infra-gravity energy compared to the gauges next to the quay. Gauge 4 shows a discrete peak at the lowest frequency range of the spectrum, thus being located close

to the antinode of the fundamental frequency. Gauges 2&3, located close to the quay of the western basin and frequently overtopped by storm waves, show peaks in higher frequencies. Therefore, these points are closer to antinodes of higher resonant modes.

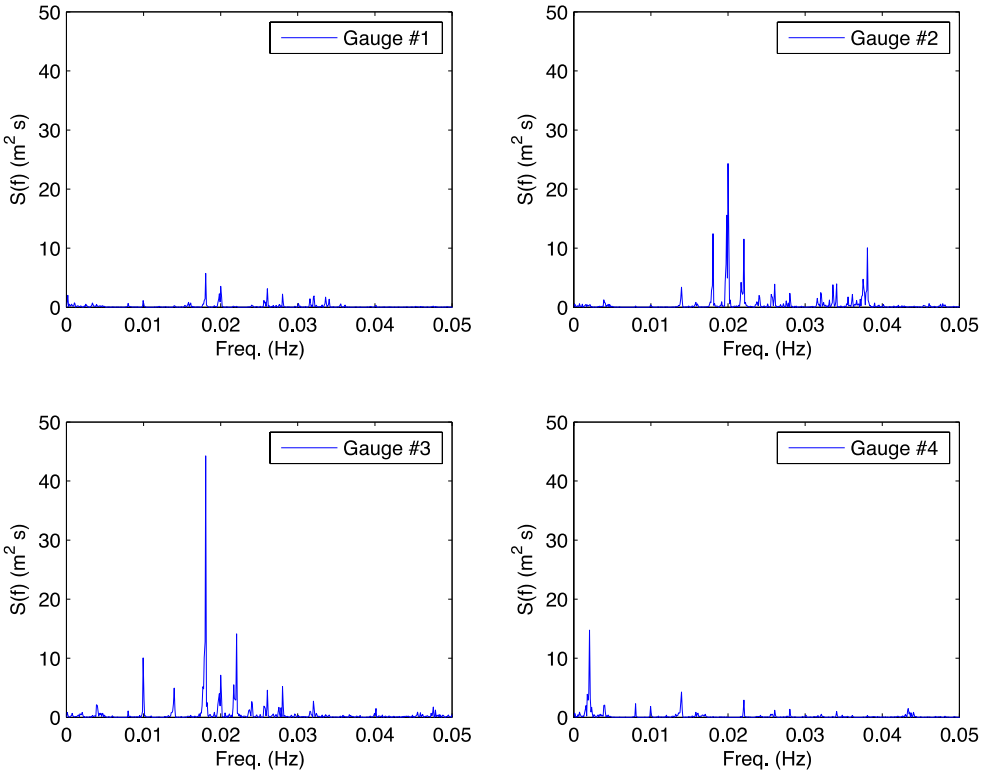

Figure 7. Raw, high-resolution spectra in the infra-gravity frequency range at locations 1-4 of Fig. 3.

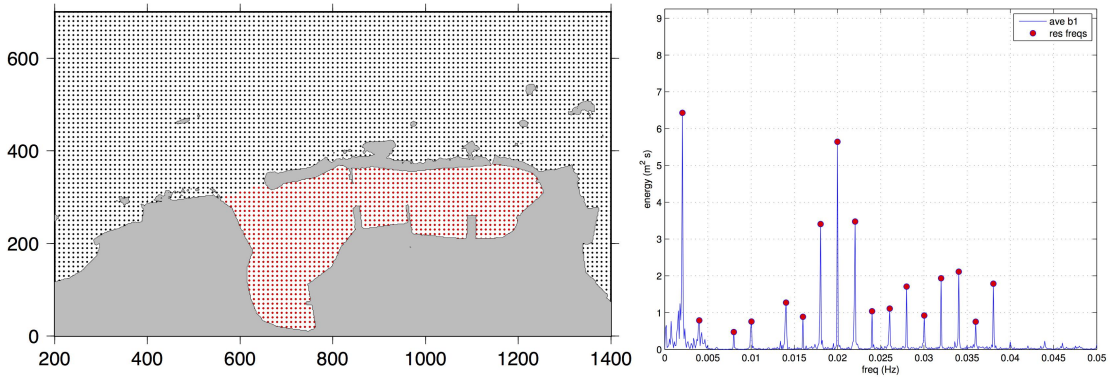

Figure 8. Left: Dots show the matrix of points for which the time-series were stored. Only red points were used for the harbor resonance spectral analysis. Right: The raw, space-averaged spectrum of the whole harbor basin. Red dots indicate the identified resonant frequencies.

To identify the resonant frequencies of the basin, we first obtain the space-averaged spectrum defined as:

$$S(f) = \frac{1}{N}\sum_{i=1}^{N} S_i(f) \qquad (1)$$

where $S_i(f)$ is the spectral energy of cell i and N is the number of wet cells in the basin. The space-averaged spectrum, combined with the inspection of the individual spectrums, provides a holistic image about the excitation of the basin. The distribution of spectral energy at each resonant frequency provides the oscillation modes. Here, instead of plotting the spectral energy distribution, we compute

the oscillation amplitude A_n for each resonant frequency, which has units of length and is easier to comprehend. The oscillation amplitude can be approximated by:

$$A_{n,j}^2 = 2\sum_{i=-p}^{p} S_{n+i,j}\Delta f \qquad (2)$$

where n is the resonant frequency number that corresponds to oscillation amplitude $A_{n,j}$ and $S_{n+I,j}$ is the spectral energy at the resonant frequency n, evaluated at point j. Spectral energy is integrated around the peak for $\pm p\Delta f$, where Δf is the frequency step, so as to approximate the wave energy corresponding the resonant frequency n. Here, we take $p = 2$.

The first four modes are shown in Fig. 9. The fundamental mode with period ~480s is defined by an antinode in the eastern end of the basin and the node at the harbor entrance. The maximum oscillation amplitude at the antinode is ~6cm. The second mode with period ~250s shows two antinodes, one at each extremity of the harbor basin, and a node roughly midway between the antinodes. The maximum oscillation amplitude at the antinode is ~2.5cm. The other two modes, with periods 125s and 100s, have the two antinodes at the basin extremities and additional in-between them.

We also examined what effect the breakwater extension design proposed in 1993 has in the resonant frequencies and respective modes (Fig. 10). Numerical modeling shows that the fundamental period is longer for the extended breakwater scenario (537s Vs 480s). The shadow zone south of the breakwater pushes the node offshore, increasing the oscillation length and stretching the oscillation period at the same time. The wave energy in the harbor decreases considerably, and so does the significant wave height. However, in terms of the long wave energy, parts of the basin exhibit significant IG energy increase with the extended breakwater. Also the oscillation amplitude maxima increase in some of the modes.

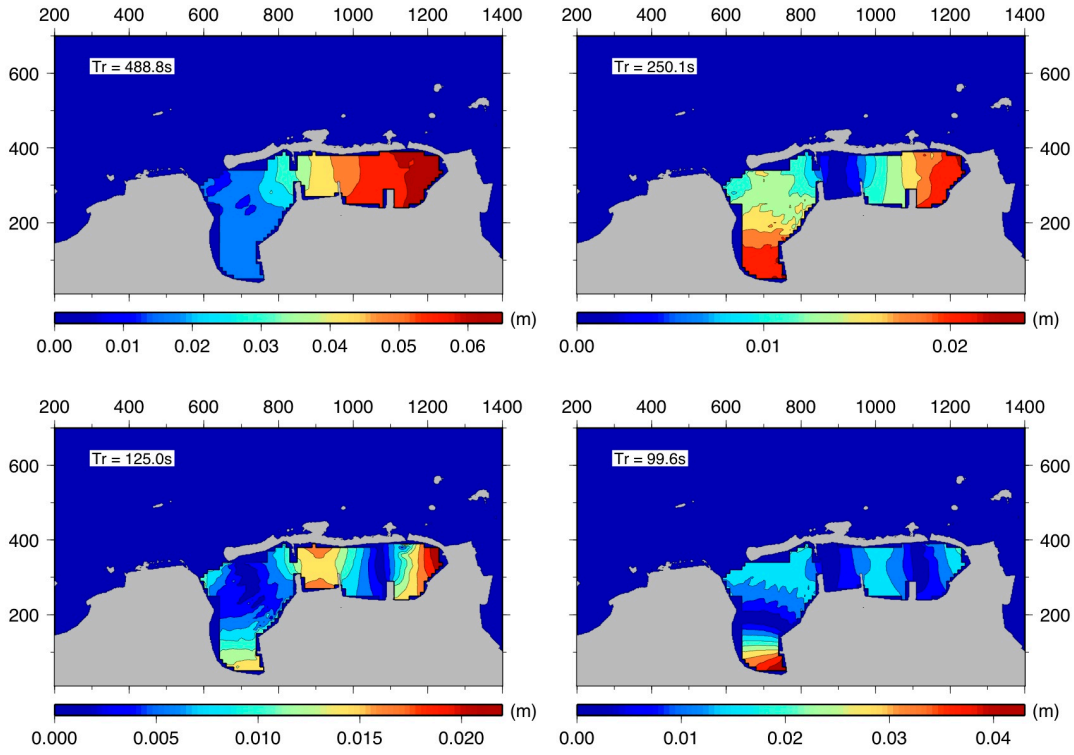

Figure 9. Harbor oscillation amplitudes of the first four modes.

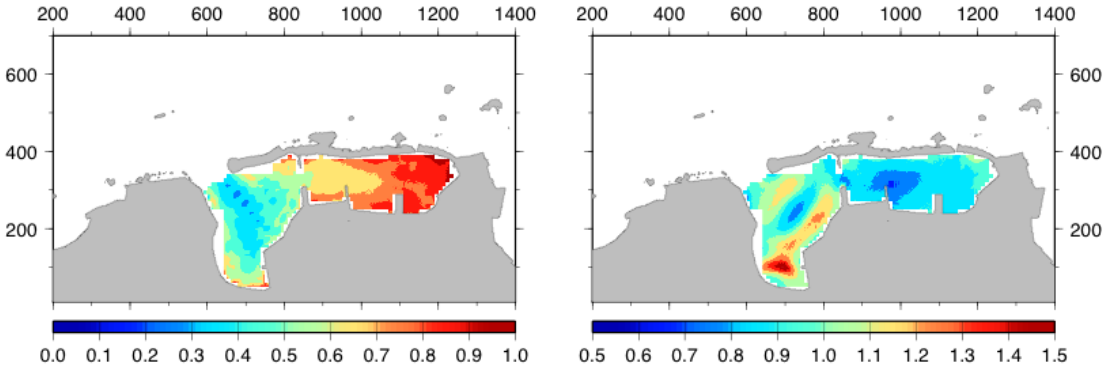

Figure 10. The ratio extended_breakwater/existing_breakwater for the total wave energy (left) and infra-gravity wave energy (right).

CONCLUSIONS

We studied resonance in the Venetian Port of Chania, a 14th century historic monument, which frequently exhibits large wave motions in its basin with flooding of its docks. We measured time histories of surface elevation and currents off the harbor for a period of two years and also measured wave elevations at one location inside the Port. The highest value of H_s since the measurements started at the study area was H_s = 4.1m with T_s = 9.2s (H_{max} in the same record was measured at 7.5m). During storm events the ratio between the significant wave height in the harbor and the one offshore might be of the order of 1/3, but values of H_s > 1m in the basin show the lack of offshore protection. We employed a Boussinesq-type model *COULWAVE* to explore resonance and determined the resonant frequencies for the entire basin. The fundamental mode with period ~480s is defined by an antinode in the eastern end of the basin and the node at the harbor entrance. The maximum oscillation amplitude at the antinode was found at ~6cm. We also explored an older proposal to extend a half-destroyed detached offshore breakwater to find how it affects wave motions in the port under storm conditions. While the wave energy is reduced, there is significant infra-gravity energy increase in different locales inside the harbor. We conclude that likely the overtopping observed under storm conditions may not be the result of harbor resonance. Substantial and professional coastal engineering needs to be undertaken to develop solutions to reduce the flooding.

ACKNOWLEDGMENTS

We acknowledge the support of the Municipal Port Fund of Chania through a contract to the Technical University of Crete (TUC), and TUC for providing the funding for the AWACs. Nikos Maravelakis is supported by the EU project ASTARTE, in the context of tsunami studies in Crete. Nikos Kalligeris is supported by USC's Myronis Fellowship.

REFERENCES

Berkhoff, J. C. W. 1972. Computation of combined refraction-diffraction, *Proc. 13th Coastal Eng. Conference,* ASCE, 471-490.

Bouws, E., H. Gunther, W. Rosenthal and C. L. Vincent. 1985. Similarity of the wind wave spectrum in finite depth water. *Journal of Geophysical Research,* 90(C1), 975-985.

Briggs, M. J., D. Dykstra and T. Baldwin. 2004. Modeling of harbor resonance in Port of Long Beach, *Proc. of International Conference on Civil Eng. in the Oceans* (edited by M. J. Briggs and M. E. McCormick), Baltimore, Maryland, USA.

Chen, H.S. and J.R. Houston. 1987. Calculation of water oscillation in coastal harbors: HARBS and HARBD user's manual, *Report CERC-87-2,* U.S. Army Waterways Experiment Station, Vicksburg, MS.

Douyere, Y.M.J. 2003. Analysis of harbor oscillation with a Boussinesq model. *MSc thesis,* University of Hawaii.

Ewing, L., C.E. Synolakis, N. Kalligeris, S. Foteinis and V. Voukouvalas. 2008. The role of regional sediment management in coastal zone management, *Proceedings of 31st International Conference on Coastal Engineering*, ASCE, 4065-4077.

Ewing, L., R.E. Flick and C.E. Synolakis. 2010. A review of coastal community vulnerabilities toward resilience benefits from disaster reduction measures, *Environmental Hazards-Human and Policy Dimensions,* 9, 222-232.

Foteinis, S. and C.E. Synolakis. 2015. Beach erosion threatens Minoan beaches: A case study of coastal retreat in Greece, *Shore and Beach* (accepted for publication).

Kazolea, M., A.I. Delis, I.K. Nikolos and C.E. Synolakis. 2012. An unstructured finite volume numerical scheme for extended Boussinesq-type equations, *Coastal Engineering*, 69, 42-66.

Kazolea, M., A.I. Delis and C.E. Synolakis. 2014. Numerical treatment of wave breaking on unstructured finite volume approximations for extended Boussinesq-type equations, *Journal of Computational Physics*, 271, 281-305.

Kofoed-Hansen, H., D. R. Kerper, O. R. Sorensen and J. Kirkegaard. 2005. Simulation of long wave agitation in ports and harbours using a time-domain Boussinesq model. *Proc. of fifth International Symposium on Ocean Wave Measurements and Analysis – WAVES, 3-7 July 2005, Madrid, Spain.*

Lepelletier, T.G. and F. Raichlen. 1987. Harbor oscillations induced by nonlinear transient long waves, *Journal of Waterway Port Coastal and Ocean Engineering-ASCE*, 113, 381-400.

Lynett, P.J. 2002. A multi-layer approach to modeling generation, propagation, and integration of water waves, PhD thesis, Cornell University.

Lynett, P. J. and P. L.-F. Liu. 2004. A two-layer approach to wave modeling. *Proc. R. Soc. Lond.,* 460, 2637-2669.

Nwogu, O .G. 1993. Alternative form of Boussinesq equations for nearshore wave propagation, *J. Waterway, Port, Coastal and Ocean Eng.*, 119(6), 618-639.

Nwogu, O. G. 2000. Time domain simulation of long period oscillations in harbors. *Coastal Engineering,* 3643-3654. doi: 10.1061/40549(276)284.

Okihiro, M., R.T. Guza and R.J. Seymour. 1993. Excitation of seiche observed in a small harbor, *Journal of Geophysical Research*, 98, 18201-18211.

Okihiro, M. and R.T. Guza. 1996. Observations of seiche forcing and amplification in three small harbors, *Journal of Waterway Port Coastal and Ocean Engineering-ASCE*, 122, 232-238.

Peregrine, D. H. 1967. Long waves on a beach, *Journal of Fluid Mechanics*, 27, pp. 815-827.

Skanavis, V., N. Kalligeris, N. Maravelakis, S. Foteinis, G. Sartzetakis, K. Papadogiannis and C.E. Synolakis. 2014. Erosion of the beaches of Crete, *AGU Fall Meeting, 15-19 December,* abstract No. OS23B-1195.

Synolakis, C.E., N. Kalligeris, S. Foteinis, and V. Voukouvalas. 2008. The Plight of the Beaches of Crete, *Proceedings of the Solutions to Coastal Disasters Conference*, Oahu, Hawaii, April 13 – 16.

Wei, G. W., J. T. Kirby, S. T. Grilli, and R. Subramanya. 1995. A fully nonlinear Boussinesq model for surface waves. Part 1. Highly nonlinear unsteady waves, *Journal of Fluid Mechanics,* 294, 71-92.